Exotic Magnetic Order in the Orbital-Selective Mott Regime of Multiorbital Systems

Julián Rincón,[1,2] Adriana Moreo,[2,3] Gonzalo Alvarez,[1,4] and Elbio Dagotto[2,3]
[1]Center for Nanophase Materials Sciences, Oak Ridge National Laboratory, Oak Ridge, Tennessee 37831, USA
[2]Materials Science and Technology Division, Oak Ridge National Laboratory, Oak Ridge, Tennessee 37831, USA
[3]Department of Physics and Astronomy, The University of Tennessee, Knoxville, Tennessee 37996, USA
[4]Computer Science & Mathematics Division, Oak Ridge National Laboratory, Oak Ridge, Tennessee 37831, USA
(Received 13 September 2013; published 11 March 2014)

The orbital-selective Mott phase of multiorbital Hubbard models has been extensively analyzed before using static and dynamical mean-field approximations. In parallel, the properties of block states (antiferromagnetically coupled ferromagnetic spin clusters) in Fe-based superconductors have also been much discussed. The present effort uses numerically exact techniques in one-dimensional systems to report the observation of block states within the orbital-selective Mott phase regime, connecting two seemingly independent areas of research, and providing analogies with the physics of double-exchange models.

DOI: 10.1103/PhysRevLett.112.106405 PACS numbers: 71.30.+h, 71.10.Fd, 71.27.+a

Introduction.—The combined interplay of charge, spin, lattice, and orbital degrees of freedom has led to an enormous variety of emergent phenomena in strongly correlated systems. A prototypical example is the half-filled single-orbital metal-insulator transition, that is realized in materials such as La_2CuO_4, a parent compound of the Cu-based high temperature superconductors. If several active orbitals are also considered in the study of this transition, an even richer phase diagram is anticipated, where states such as band insulators, correlated metals, and orbital-selective Mott phases (OSMP) can be stabilized. In particular, the study of the OSMP and its associated orbital-selective Mott transition has attracted considerable attention in recent years [1–3].

The OSMP is a state where even though Mott insulator (MI) physics occurs, it is restricted to a subset of all the active orbitals present in the problem. This state has narrow-band localized electrons related to the MI orbitals, coexisting with wideband itinerant electrons at the other orbitals [4–6]. To stabilize the OSMP, a robust Hund interaction J is needed. In general, the hybridization within orbitals γ, $V_{\gamma,\gamma'}$, and crystal fields Δ_γ work against J since they favor low-spin ground states. Therefore, if $J \gg \Delta_\gamma$, $V_{\gamma,\gamma'}$, the OSMP is expected to be stable and display robust local moments [6].

Several studies focused on the effects of interactions, filling fractions, etc., on the stability of orbital-selective phases [3]. This previous theoretical work was performed within mean-field approximations (such as dynamical mean field theory [4–8], slave spins [6,8–11], or Hartree-Fock [12,13]). Using these methods the OSMP stability conditions have been established. However, to our knowledge, there have been no detailed studies of the influence of full quantum fluctuations on this phase and therefore, and more importantly for our purposes, of their low-temperature electronic and magnetic properties.

Recently, these issues received considerable attention in the Fe-based superconductors community. In this context, multiorbital models containing Hubbard U and J interactions, as well as crystal-field splittings, are widely employed, and the existence of OSMP regimes has been extensively investigated [6,7,9,10,12–17]. For these reasons, our models are chosen to resemble qualitatively models for pnictides and selenides, so that our conclusions could be of potential relevance in that context.

Our aim is twofold: (i) By employing techniques beyond mean field to study the phase diagrams of three-orbital Hubbard models, the robustness of the OSMP to full quantum fluctuations can be confirmed via numerical simulations; (ii) more importantly, once the stability of this state has been established, its charge and magnetic orders can be explored. Our main result is that full ferromagnetic (FM) and exotic "block" states have been found to be stable within the OSMP regime. Block phases, such as the antiferromagnetic (AFM) state made of 2×2 FM clusters, were discussed extensively in the selenides literature mainly in the presence of iron vacancies [18–26] or in special geometries such as two-leg ladders [27–29], but not in the OSMP framework. Our new results suggest that the concepts of OSMP and block phases, until now separately considered, are actually related after showing that block states are stabilized *within* the OSMP regime.

Our study is performed in a one-dimensional geometry. This restriction arises from the need to employ accurate techniques such as the density matrix renormalization group (DMRG) [30–32]. Thus, our conclusions are only *suggestive* of similar physics in the layered Fe-based superconductors, and only further work can confirm this assumption. However, there are real quasi-one-dimensional materials, such as the previously mentioned ladders [27–29], that may provide a direct physical realization of our results.

 © 2014 American Physical Society

Model.—The Hamiltonians used are multiorbital Hubbard models composed of kinetic energy and interacting terms: $H = H_K + H_{\rm int}$. The kinetic contribution is written as

$$H_K = -\sum_{i\sigma\gamma\gamma'} t_{\gamma\gamma'}(c^+_{i\sigma\gamma}c_{i+1\sigma\gamma'} + \text{H.c.}) + \sum_{i\sigma\gamma}\Delta_\gamma n_{i\sigma\gamma}, \quad (1)$$

where $t_{\gamma\gamma'}$ denotes a (symmetric) hopping amplitude defined in orbital space $\{\gamma\}$ connecting the lattice sites i and $i+1$ ($\gamma = 0,\ 1,\ 2$) of a one-dimensional lattice of length L. The hopping amplitudes used here are (eV units): $t_{00} = t_{11} = -0.5$, $t_{22} = -0.15$, $t_{02} = t_{12} = 0.1$, and $t_{01} = 0$, with an associated total bandwidth $W = 4.9|t_{00}|$ (the individual orbital bandwidths $W_\gamma/|t_{00}|$ are 3.69, 3.96, and 1.54, for $\gamma = 0$, 1, and 2, respectively). Both hoppings and W are comparable in magnitude to those used in more realistic pnictides models [33]. Only hybridizations between orbitals 0 and 2, and 1 and 2, are considered. Δ_γ defines a crystal-field splitting which is orbital dependent with values $\Delta_0 = -0.1$, $\Delta_1 = 0$, and $\Delta_2 = 0.8$. All these parameters are *phenomenological*, i.e., not derived from *ab initio* calculations. Their values were chosen so that the band structure [shown in the inset of Fig. 2(a)] qualitatively resembles that of higher dimensional pnictides, with a hole pocket at $k = 0$ and electron pockets at $k = \pm\pi$. This model will be referred to as "Model 1" while a "Model 2" with slightly different parameters will be discussed in the Supplemental Material [34]. The Coulombic repulsion interacting portion of the Hamiltonian is

$$H_{\rm int} = U\sum_{i\gamma} n_{i\uparrow\gamma}n_{i\downarrow\gamma} + (U' - J/2)\sum_{i\gamma<\gamma'} n_{i\gamma}n_{i\gamma'} - 2J\sum_{i\gamma<\gamma'}\mathbf{S}_{i\gamma}\cdot\mathbf{S}_{i\gamma'} + J\sum_{i\gamma<\gamma'}(P^+_{i\gamma}P_{i\gamma'} + \text{H.c.}), \quad (2)$$

containing the standard intraorbital Hubbard repulsion U, and Hund's rule coupling J. For SU(2) symmetric systems, the relation $U' = U - 2J$ holds. $c_{i\sigma\gamma}$ annihilates an electron with spin σ at orbital γ and site i, and $n_{i\sigma\gamma}$ counts electrons at i with quantum numbers (σ, γ) The operator $\mathbf{S}_{i\gamma}$ ($n_{i\gamma}$) is the spin (total electronic density) at orbital γ and site i, and the definition $P_{i\gamma} = c_{i\downarrow\gamma}c_{i\uparrow\gamma}$ was introduced. The electronic density per orbital is fixed to $n = 4/3$, i.e., four electrons every three orbitals, in analogy with the filling used in the modeling of iron superconductors with three orbitals [33]. As a many-body technique, the DMRG method [30–32] was used, with technical details provided in the Supplemental Material [34].

Results.—In Fig. 1, the phase diagram of Model 1 is shown, based on the DMRG measurements of the orbital occupancies n_γ and the square of the spin operator at every site (see Fig. 2). Two phases are obvious: a metallic weakly interacting state M at small U and a MI regime at large U,

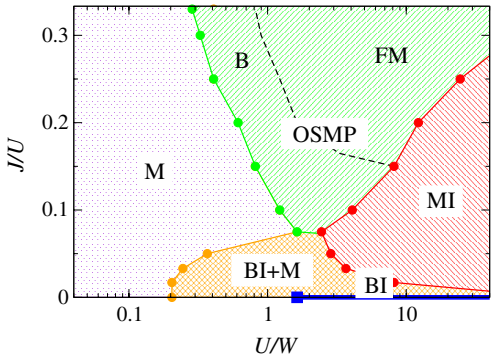

FIG. 1 (color online). Phase diagram of the three-orbital Model 1 for $n = 4/3$. The different phases are labeled as follows: metal (M), band insulator (BI), a metallic state resembling the BI state (BI + M), Mott insulator (MI), and orbital-selective Mott phase (OSMP). Within the OSMP regime, it is possible to distinguish between block (B) and FM states.

where $n_0 = 2$, $n_1 = n_2 = 1$ minimize the double-occupancy energy penalization and J induces a spin 1 state at each site (orbital 0 is doubly occupied because of the small but nonzero split between orbitals 1 and 0). Naturally, the spin order is staggered in the MI phase. Less obvious are the other two phases in Fig. 1. For example, a correlated "band insulator" (BI) with $n_0 = n_1 = 2$ and $n_2 = 0$ is found in a region bounded by J less than the crystal-field splittings Δ_γ, so that the low-spin state is favored, and U/W not too large, so that double occupancy is not heavily suppressed by U. At J exactly 0.0, the BI state survives for any value of U/W because in this line $U = U'$. But at large U/W, a tiny J is sufficient to destabilize the BI state into the MI state. The related BI + M state has $n_0 \sim n_1 \sim 2$ and $n_2 \sim 0$: a metallic state with characteristics close to the BI [35]. Clearly, increasing J/U the BI/BI + M phases are suppressed. In fact, with increasing U/W the M state is the most stable at $J/U \sim 0.075$ because of the competition J vs Δ_γ. Since the BI/BI + M states are not our main focus, additional properties are in the Supplemental Material [34].

Our most important result in Fig. 1 is the presence of a prominent OSMP regime, stabilized after J becomes larger than a threshold that depends on Δ_γ. The OSMP contains the region $J/U \sim 1/4$ at intermediate U/W believed to be realistic [36–39]. For the prototypical value $J/U = 1/4$, in the small-U metallic regime the n_γ values evolve smoothly from the noninteracting limit. However, at a critical U/W, the $\gamma = 2$ orbital population reaches 1 and stays there in a wide window of couplings, while the other two densities develop a value ~1.5 [Fig. 2(a)]. These results are robust against changes in L and they are compatible with the presence of an OSMP, that eventually ends at a second critical U/W when the transition to the MI regime occurs. In the Supplemental Material [34], results similar to Fig. 2(a) but adding two holes are shown: while n_2 remains at 1 in the OSMP regime, now $n_0 \sim n_1 \sim 1.37$, showing that

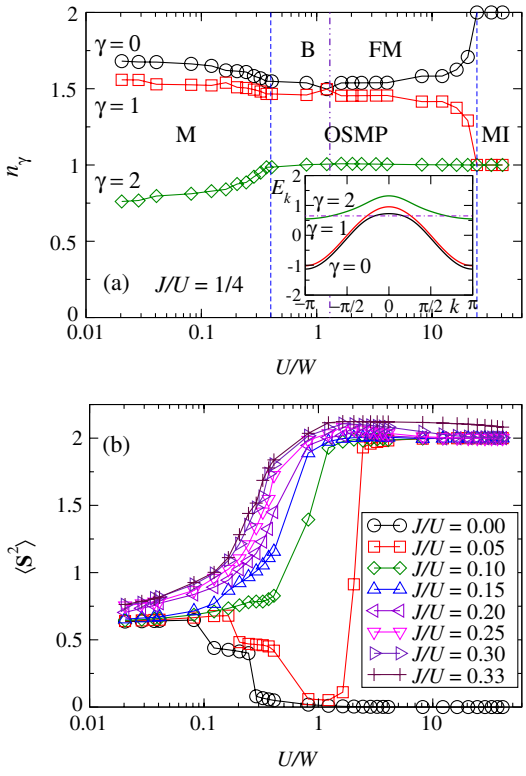

FIG. 2 (color online). Results for Model 1: (a) Electronic occupancy n_γ corresponding to orbital γ vs U in bandwidth W units, at $J/U = 1/4$, and for $L = 24$. Inset: Band structure of Model 1 (eV units). Violet (dash-dotted) line is the $n = 4/3$ Fermi level. (b) Mean value of the square of the total spin at each site, at several values of J/U. Within the OSMP, a robust magnetic moment is observed.

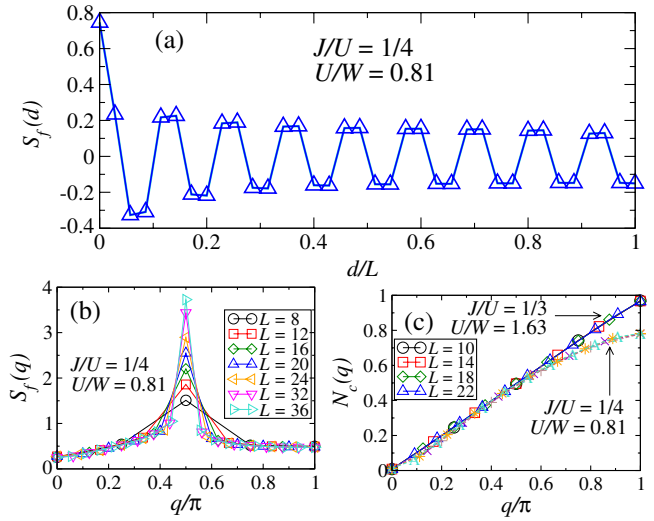

FIG. 3 (color online). (a) Spin correlations in the localized (insulating) band vs the normalized distance, at $J/U = 1/4$, $U/W = 0.81$, and $L = 36$. The formation of ferromagnetic clusters interacting antiferromagnetically is clearly shown. (b) Spin structure factor for panel (a) at several L's (symbols). A clear peak at $q/\pi = 1/2$ is shown. (c) Charge structure factor of the itinerant bands for the J/U and U/W indicated, and varying L (symbols).

n_0 and n_1 evolve with doping while n_2 is locked as expected in the OSMP [40]. The formation of a robust local moment in the OSMP is shown in Fig. 2(b). These DMRG results confirm the presence of the OSMP even with full quantum fluctuations incorporated. The OSMP regime is eventually suppressed by decreasing J/U: at weak U/W coupling because of the competition with Δ_γ that favors the M and BI + M states, and at strong U/W coupling because of the competition with the MI state.

While previous mean-field studies of the OSMP arrive to conclusions qualitatively similar to those of Fig. 2, the DMRG method can reveal the fine details of the OSMP spin and charge arrangements. For example, Fig. 3(a) contains representative OSMP spin-spin correlation functions [34]. Surprisingly, an unexpected pattern of spins $\uparrow\uparrow\downarrow\downarrow$ is clearly observed. The spin structure factor in Fig. 3(b) displays a sharp peak at $q = \pi/2$, that increases with L (the peak is also robust away from $n = 4/3$). Then, at intermediate couplings, our DMRG results indicate that exotic block spin states can be stabilized within the OSMP (region "B" in Fig. 1). These block spin states are qualitatively similar to those reported for pnictides and selenides [18–29].

In addition, a surprising FM OSMP region with a maximal value of the spin has been found (see Supplemental Material [34]). Its charge structure factor $N_c(q)$ is shown in Fig. 3(c) at several L's. Although there are no signs of charge order, there is clear evidence of spinless fermions behavior with momentum $q = \pi$. The effective filling of the emergent spinless fermions can be understood by considering that there are three electrons per site in the itinerant bands (and one in the localized band). This is equivalent to one hole per site per two orbitals or, equivalently, $1/2$ hole per site on an effective chain of length $2L$. This is a "half-filled" spinless fermion system, inducing the momentum of π in $N_c(q)$. For the B phase, $N_c(q)$ shows a qualitatively similar behavior, no charge order, and a spectrum broadening as shown in Fig. 3(c) [34].

Figure 4(a) shows the finite-size dependence of the peak of the charge and spin structure factors, generically referred to as $F_x(q_{\max})$, for the B and FM regions. F_x becomes S_f and N_c for spin and charge, respectively, at the maximal momentum $q_{\max}$. The FM state displays a quasilinear increase of the structure factor peak vs L signaling a quasi-long-range order in the spin correlations. The B phase presents a logarithmic increase with L indicating, again, (quasi-long-ranged) power-law behavior of the spin correlations with nontrivial exponents [see inset Fig. 4(a)]. On the other hand, the charge peak shows no order tendencies in any of the phases evidencing only short-ranged correlations; however, the charge correlations show

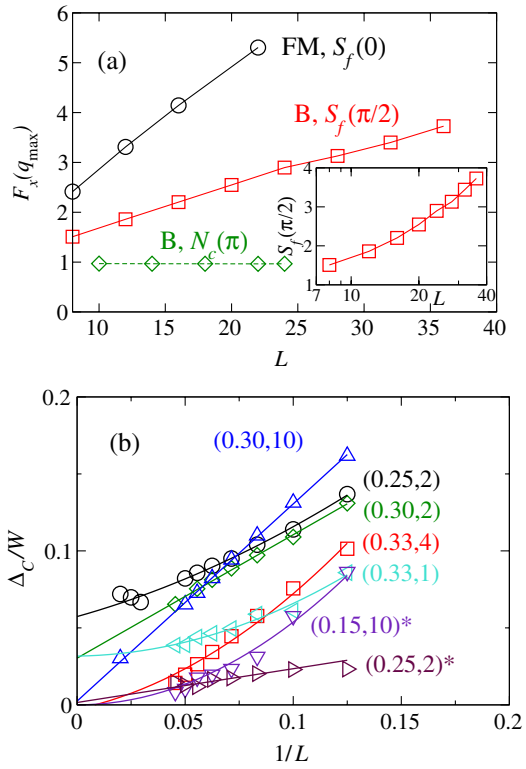

FIG. 4 (color online). (a) Size dependence of the peaks of the charge (dashed line) and spin (solid line) structure factors for the FM and B phases with couplings $J/U = 1/4$, $U/W = 0.81$ and $J/U = 1/3$, $U/W = 1.63$, respectively. Inset: Semilogarithmic plot of $S_f(\pi/2)$. (b) Charge gap vs $1/L$ for the values of the pair $(J/U, U)$ shown. Results with the * symbol stand for the 2-hole doped case.

a nontrivial trend associated with spinless behavior, as discussed in Fig. 3(c).

The metallic vs insulating nature of the OSMP is difficult to address, but guidance can be obtained by studying the charge gap Δ_C [34] [see Fig. 4(b)]. While the extrapolation to the bulk is difficult, "by eye" it is clear that the extrapolations appear to converge to small gaps in the $0.05 \times W$ to 0.00 range. Moreover, upon light 2-hole doping the gap vanishes. Thus, a likely scenario is that the block states at exactly $n = 4/3$ have a small gap that rapidly closes with doping. Since in the realistic five-orbital Hubbard model for pnictides the combined population of the xz, yz, and xy orbitals is not exactly 4, the relevant OSMP regime would be metallic.

Relation to Kondo lattice models.—The results reported here unveil interesting analogies with previous studies of the double-exchange (DE) models for Mn oxides [41]. This is natural, since DE physics relies on the interplay of localized and itinerant degrees of freedom, as it occurs in the OSMP regime. This DE-OSMP relation is rigorous: for the case of a two-band model, it has been shown that the low-energy effective theory of the OSMP is related to a FM Kondo lattice model with Hubbard repulsion in the conduction band [5]. For a generic multiorbital case, one can show that the effective model turns into a "correlated" FM Kondo lattice model. If the system has $n_{\rm orb}$ orbitals, this model describes the FM exchange between the localized band with magnetic moments and a many-body bath of itinerant electrons. The bath is built out of the remaining $n_{\rm orb} - 1$ orbitals and the only interaction between localized and itinerant bands is the FM exchange.

This DE-OSMP relation provides further support to the main conclusions of our effort. In fact, previous DMRG and Monte Carlo investigations of the DE model already unveiled a variety of so-called "island phases" containing small clusters of various shapes made of ferromagnetically aligned spins and with AFM couplings among them, both in one and two dimensions [42–45]. These phases are qualitatively the analog of the block phases, although for quite different couplings, electronic densities, and band structures. The previous DE results [42–45] reinforce our conjecture that the block states observed here via the detailed analysis of examples are likely stable for a wider variety of models, both in one and two dimensions. Since in manganites it was shown that exotic non-FM phases need the crucial addition of a superexchange coupling $J_{\rm AFM}$ between the localized spins [41,46,47], it is natural to conjecture that a similar coupling must be incorporated into the effective model in the OSMP regime of iron superconductors and related compounds.

Conclusions.—In this Letter, multiorbital Hubbard models have been investigated using DMRG techniques in one dimension, and the phase diagrams have been constructed. Our main result is that the OSMP regime contains unexpected internal structure. In particular, phases with the characteristics of block states (FM clusters, AFM coupled) have been identified. Full FM has also been found within the OSMP. The block states likely arise from the frustration generated by competing ferromagnetic and antiferromagnetic tendencies in the model, as it happens with the island phases in manganites. Block phases were discussed before in models of Fe-based superconductors, but were not associated with the OSMP regime. Moreover, since a formal mapping between the Hubbard and Kondo lattice models exists in the OSMP regime, our results establish an unexpected analogy between double-exchange physics, where similar block phases were reported before, and that of multiorbital models for iron superconductors. Our conclusions are of direct relevance to real quasi-one-dimensional materials but they may apply to two-dimensional systems as well, considering that "island phases" in the two-dimensional Kondo models have been reported before [45].

Support by the Early Career Research Program, Scientific User Facilities Division, Basic Energy Sciences, U.S. Department of Energy, under contract with UT-Battelle (J. R. and G. A.) and by the U.S. Department of Energy, Office of Basic Energy Sciences, Materials

Sciences and Engineering Division (J. R.) is acknowledged. For this project, A. M. and E. D. were supported by the National Science Foundation under Grant No. DMR-1104386.

[1] V. I. Anisimov, I. A. Nekrasov, D. E. Kondakov, T. M. Rice, and M. Sigrist, Eur. Phys. J. B **25**, 191 (2002).
[2] M. Vojta, J. Low Temp. Phys. **161**, 203 (2010).
[3] A. Georges, L. de' Medici, and J. Mravlje, Annu. Rev. Condens. Matter Phys. **4**, 137 (2013).
[4] A. Liebsch, Phys. Rev. B **70**, 165103 (2004).
[5] S. Biermann, L. de' Medici, and A. Georges, Phys. Rev. Lett. **95**, 206401 (2005).
[6] L. de' Medici, S. R. Hassan, M. Capone, and X. Dai, Phys. Rev. Lett. **102**, 126401 (2009).
[7] H. Ishida and A. Liebsch, Phys. Rev. B **81**, 054513 (2010).
[8] L. de' Medici, Phys. Rev. B **83**, 205112 (2011).
[9] R. Yu and Q. Si, Phys. Rev. B **86**, 085104 (2012).
[10] R. Yu and Q. Si, Phys. Rev. Lett. **110**, 146402 (2013).
[11] L. de' Medici, G. Giovannetti, and M. Capone, arXiv:1212.3966.
[12] E. Bascones, B. Valenzuela, and M. J. Calderón, Phys. Rev. B **86**, 174508 (2012).
[13] B. Valenzuela, M. J. Calderón, G. León, and E. Bascones, Phys. Rev. B **87**, 075136 (2013).
[14] A. Liebsch, Phys. Rev. B **84**, 180505(R) (2011).
[15] M. Yi, D. H. Lu, R. Yu, S. C. Riggs, J.-H. Chu, B. Lv, Z. K. Liu, M. Lu, Y. T. Cui, M. Hashimoto, S.-K. Mo, Z. Hussain, C.-W. Chu, I. R. Fisher, Q. Si, and Z.-X. Shen, Phys. Rev. Lett. **110**, 067003 (2013).
[16] N. Lanatá, H. U. R. Strand, G. Giovannetti, B. Hellsing, L. de' Medici, and M. Capone, Phys. Rev. B **87**, 045122 (2013).
[17] M. Greger, M. Kollar, and D. Vollhardt, Phys. Rev. Lett. **110**, 046403 (2013).
[18] W. Bao, Q. Huang, G. F. Chen, M. A. Green, D. M. Wang, J. B. He, X. Q. Wang, and Y. Qiu, Chin. Phys. Lett. **28**, 086104 (2011).
[19] C. Cao, and J. Dai, Phys. Rev. Lett. **107**, 056401 (2011).
[20] Q. Luo, A. Nicholson, J. Riera, D.-X. Yao, A. Moreo, and E. Dagotto, Phys. Rev. B **84**, 140506(R) (2011).
[21] R. Yu, J.-X. Zhu, and Q. Si, Phys. Rev. Lett. **106**, 186401 (2011).
[22] S.-M. Huang and C.-Yu Mou, Phys. Rev. B **84**, 184521 (2011).
[23] W. Li, S. Dong, C. Fang, and J.-P. Hu, Phys. Rev. B **85**, 100407(R) (2012).
[24] W.-G. Yin, C.-C. Lee, and W. Ku, Phys. Rev. Lett. **105**, 107004 (2010).
[25] E. Dagotto, Rev. Mod. Phys. **85**, 849 (2013), and references therein.
[26] P. Dai, J. P. Hu, and E. Dagotto, Nat. Phys. **8**, 709 (2012).
[27] J. M. Caron, J. R. Neilson, D. C. Miller, A. Llobet, and T. M. McQueen, Phys. Rev. B **84**, 180409(R) (2011).
[28] J. M. Caron, J. R. Neilson, D. C. Miller, K. Arpino, A. Llobet, and T. M. McQueen, Phys. Rev. B **85**, 180405(R) (2012).
[29] Q. Luo, A. Nicholson, J. Rincón, S. Liang, J. Riera, G. Alvarez, L. Wang, W. Ku, G. D. Samolyuk, A. Moreo, and E. Dagotto, Phys. Rev. B **87**, 024404 (2013).
[30] S. R. White, Phys. Rev. Lett. **69**, 2863 (1992); Phys. Rev. B **48**, 10345 (1993).
[31] U. Schollwöck, Rev. Mod. Phys. **77**, 259 (2005).
[32] K. Hallberg, Adv. Phys. **55**, 477 (2006).
[33] M. Daghofer, A. Nicholson, A. Moreo, and E. Dagotto, Phys. Rev. B **81**, 014511 (2010).
[34] See Supplemental Material at http://link.aps.org/supplemental/10.1103/PhysRevLett.112.106405 for details of the definition of physical quantities, and additional numerical results.
[35] This BI + M phase (not to be confused with a phase separated state involving the BI and M states) has characteristics similar to those reported at small J in R. Yu and Q. Si, Phys. Rev. B **84**, 235115 (2011). Further studies beyond the scope of the present publication can clarify its properties, as well as the true existence of a sharp transition between the M and **BI + M** states.
[36] K. Haule and G. Kotliar, New J. Phys. **11**, 025021 (2009).
[37] Q. Luo, G. Martins, D.-X. Yao, M. Daghofer, R. Yu, A. Moreo, and E. Dagotto, Phys. Rev. B **82**, 104508 (2010).
[38] Z. P. Yin, K. Haule, and G. Kotliar, Nat. Mater. **10**, 932 (2011).
[39] J. Ferber, K. Foyevtsova, R. Valentí, and H. O. Jeschke, Phys. Rev. B **85**, 094505 (2012); see also Y.-Z. Zhang, H. Lee, H.-Q. Lin, C.-Q. Wu, H. O. Jeschke, and R. Valentí, Phys. Rev. B **85**, 035123 (2012), and references therein.
[40] The inset of Fig. S6 in the Supplemental Material [34] shows that n_0 and n_1 are very close in the OSMP regime, but not identical. The same occurs in Fig. 2(a). The reason is that the initial small energy splitting between levels 0 and 1 is washed out in the OSMP where U/W is of order 1 or larger.
[41] E. Dagotto, T. Hotta, and A. Moreo, Phys. Rep. **344**, 1 (2001).
[42] D. J. García, K. Hallberg, C. D. Batista, M. Avignon, and B. Alascio, Phys. Rev. Lett. **85**, 3720 (2000).
[43] D. J. Garcia, K. Hallberg, C. D. Batista, S. Capponi, D. Poilblanc, M. Avignon, and B. Alascio, Phys. Rev. B **65**, 134444 (2002).
[44] D. J. Garcia, K. Hallberg, B. Alascio, and M. Avignon, Phys. Rev. Lett. **93**, 177204 (2004).
[45] H. Aliaga, B. Normand, K. Hallberg, M. Avignon, and B. Alascio, Phys. Rev. B **64**, 024422 (2001).
[46] S. Yunoki and A. Moreo, Phys. Rev. B **58**, 6403 (1998).
[47] A. Moreo, M. Mayr, A. Feiguin, S. Yunoki, and E. Dagotto, Phys. Rev. Lett. **84**, 5568 (2000).